

# SpiritSight Agent: Advanced GUI Agent with One Look

Zhiyuan Huang<sup>1\*</sup> Ziming Cheng<sup>1,2\*</sup> Junting Pan<sup>3</sup> Zhaohui Hou<sup>1</sup> Mingjie Zhan<sup>1</sup>  
<sup>1</sup>SenseTime Research, <sup>2</sup>Beijing University of Posts and Telecommunications, <sup>3</sup>MMLab, CUHK

## Abstract

Graphical User Interface (GUI) agents show amazing abilities in assisting human-computer interaction, automating human user’s navigation on digital devices. An ideal GUI agent is expected to achieve high accuracy, low latency, and compatibility for different GUI platforms. Recent vision-based approaches have shown promise by leveraging advanced Vision Language Models (VLMs). While they generally meet the requirements of compatibility and low latency, these vision-based GUI agents tend to have low accuracy due to their limitations in element grounding. To address this issue, we propose **SpiritSight**, a vision-based, end-to-end GUI agent that excels in GUI navigation tasks across various GUI platforms. First, we create a multi-level, large-scale, high-quality GUI dataset called **GUI-Lasagne** using scalable methods, empowering SpiritSight with robust GUI understanding and grounding capabilities. Second, we introduce the **Universal Block Parsing (UBP)** method to resolve the ambiguity problem in dynamic high-resolution of visual inputs, further enhancing SpiritSight’s ability to ground GUI objects. Through these efforts, SpiritSight agent outperforms other advanced methods on diverse GUI benchmarks, demonstrating its superior capability and compatibility in GUI navigation tasks. Models are available at <https://huggingface.co/SenseLLM/SpiritSight-Agent-8B>.

## 1. Introduction

Graphical User Interface (GUI) automation has long been pursued by people along with the development of the modern digital devices. Thanks to recent advances in Large Language Models (LLMs), GUI agents are constructed to assist users in interacting with graphical interfaces, automatically making action decisions based on observations of environment and user’s instruction.

Current approaches can be divided into three categories based on their input modalities. Language-based and

\*Equal contribution.

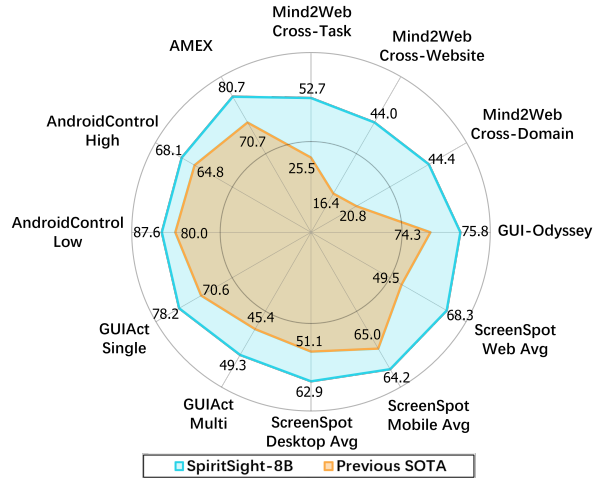


Figure 1. Our SpiritSight agent achieves new state-of-the-art (SOTA) performance across various benchmarks in web, mobile, and desktop scenarios.

vision-based approaches use Hyper Text Markup Language (HTML) or Extensible Markup Language (XML) and screenshots as input [7, 11, 13, 19, 22, 26, 28, 53, 68, 75], respectively, while vision-language-based approaches combine both HTML and screenshots as input [15, 24, 52, 74].

The language-based and vision-language-based methods typically applied only in the web domain, and often limited by the excessive length of HTML or security concerns [34, 61, 71] regarding it. The vision-based approaches exhibit compatibility across various GUI platforms, as acquiring screenshots is generally easier than obtaining hierarchical data from non-web platforms.

However, vision-based approaches struggle to ground GUI elements (e.g. buttons, text boxes) from the visual input [74]. Some works solve this problem by introducing additional tools, such as optical character recognition (OCR) and icon recognition models, to convert the visual grounding task into a language QA task [55, 56]. This may increase the complexity and inference latency of the agent system. Others attempt to collect large-scale training data

through manual synthesis [27, 36, 51] or human annotation [5, 6, 13, 38, 39, 46, 65], while these data are either unrealistic or costly. Additionally, recent advanced Vision Language Models (VLMs) [9, 67] adopt dynamic high-resolution [9, 67] strategy to better suit high-resolution inputs, which we find may introduce ambiguity to the model learning process in GUI scenarios.

To address the aforementioned challenges, we proposed an end-to-end, vision-based GUI agent—SpiritSight, which has strong ability in GUI navigation task. Our contributions are summarized as follows:

**Firstly, we propose GUI-Lasagne, a multi-level, large-scale and high-quality GUI dataset composed of 5.73 million samples to enhance our model’s GUI understanding and grounding capabilities.** The dataset is collected from the real-world and filtered through carefully designed rules to ensure data quality. It is also constructed hierarchically and consists of three levels of components: text/icon recognition and grounding data, function grounding data, and GUI navigation data. The first two parts constitute 90% of the total dataset and are collected for free, thus significantly reducing the data collection cost.

**Secondly, We introduce a Universal Block Parsing (UBP) method to resolve the ambiguity problem in dynamic high-resolution inputs.** With the effectiveness of UB, SpiritSight gains an improved elements grounding capability and achieves significant performances in GUI navigation tasks.

**Thirdly, we release and evaluate SpiritSight agent in various GUI benchmarks and it exhibits impressive performance among them.** SpiritSight agent is pre-trained on GUI-Lasagne dataset and employs UB method to ground target elements, as shown in Fig. 3. We release three versions of SpiritSight with different model size: SpiritSight-26B, SpiritSight-8B, and SpiritSight-2B. The standard SpiritSight-8B consistently outperforms previous state-of-the-art methods across various GUI benchmarks, as shown in Fig. 1. On the Multimodal-Mind2Web [13] benchmark, the SpiritSight series outperforms all kinds of methods—including language-based, vision-based and even vision-language-based methods—in the non-candidate setting, as shown in Fig. 2.

## 2. Related Works

### 2.1. Language-based and vision-language-based GUI Agent

Several works leverage the capabilities of large-scale language models (LLMs) to construct GUI agents. It is noticed that they are mostly multi-stage architectures. Mind2Web [13] utilizes a lightweight language model to extract candidate elements from HTML, followed by a ranking model that sorts these elements based on task descriptions

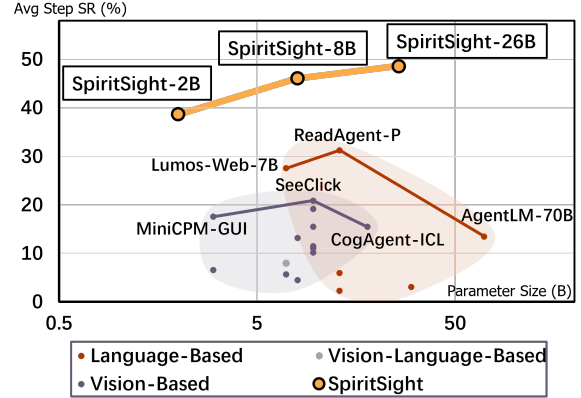


Figure 2. Comparison of the average step success rate on Multimodal-Mind2Web benchmark of our SpiritSight agent of three sizes (2B, 8B, 26B) with various previous methods.

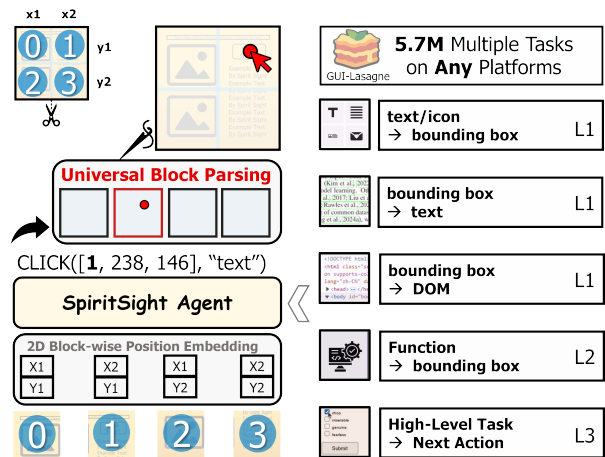


Figure 3. The overview of our SpiritSight agent. We develop a large-scale, multi-level, high-quality pre-training dataset that equips SpiritSight with three levels of comprehensive GUI knowledge. Additionally, we introduce a Universal Block Parsing (UBP) method to enhance SpiritSight’s grounding capabilities.

and historical actions. Finally, a large language model predicts the current actions and selects the target elements to operate on. WebAgent [17] first uses an encoder-decoder model to generate low-level instructions and relevant HTML code snippets, then uses another decoder to produce executable Python code. AutoWebGLM [26] simplifies HTML code through manually designed rules before predicting the executable action codes.

Other vision-language-based works leverage both GUI screenshots and hierarchical HTML/XML to enhance the robustness of GUI agents. WebGUM [15] and CC-Net [52] use ResNet and ViT to extract features from screenshots, respectively. The image embeddings are then combined with text embeddings and fed into a multi-modal transformer. See-

	Model Size	Input Modality	Select From Top	Cross-Task			Cross-Website			Cross-Domain		
				Ele.Acc	Op.F1	Step SR	Ele.Acc	Op.F1	Step SR	Ele.Acc	Op.F1	Step SR
AutoWebGLM [26]	6B	Text	✓	-	-	66.4%	-	-	56.4%	-	-	55.8%
LLaMA2-7B [26]	7B	Text	✓	-	-	52.7%	-	-	47.1%	-	-	50.3%
CogAgent [19]	18B	Image	✓	-	-	62.3%	-	-	54.0%	-	-	59.4%
HTML-T5-XL [17]	3B	Text	✓	76.4%	78.8%	71.5%	68.4%	71.0%	62.2%	73.0%	75.6%	67.1%
SeeAct [74]	-	Text+Image	×	46.4%	73.4%	40.2%	38.0%	67.8%	32.4%	42.4%	69.3%	36.8%
ReadAgent-P [28]	340B	Text	×	33.7%	72.5%	29.2%	37.4%	75.1%	31.1%	37.2%	76.3%	33.4%
MiniCPM-GUI [7]	3B	Image	×	23.8%	86.8%	20.8%	20.3%	81.7%	17.3%	17.9%	74.5%	14.6%
Fuyu-GUI [4]	8B	Image	×	19.1%	86.1%	15.6%	13.9%	80.7%	12.2%	14.2%	83.1%	11.7%
SeeClick [11]	9.6B	Image	×	28.3%	87.0%	25.5%	21.4%	80.6%	16.4%	23.2%	84.8%	20.8%
OmniParser [53]	-	Image	×	42.4%	87.6%	39.4%	41.0%	84.8%	36.5%	45.5%	85.7%	42.0%
SpiritSight-2B	2B	Image	×	51.7%	87.2%	44.9%	44.0%	83.6%	37.8%	42.4%	83.5%	36.9%
SpiritSight-8B	8B	Image	×	59.2%	88.9%	52.7%	52.2%	84.7%	44.0%	50.1%	86.0%	44.4%
SpiritSight-26B	26B	Image	×	<b>60.5%</b>	<b>89.7%</b>	<b>54.7%</b>	<b>57.0%</b>	<b>85.7%</b>	<b>48.1%</b>	<b>54.1%</b>	<b>87.2%</b>	<b>49.2%</b>

Table 1. Comparison of SpiritSight agent with various previous methods on Multimodal-Mind2Web benchmark. SpiritSight significantly outperforms all methods that do not rely on any candidate element, including vision-based methods, language-based methods, and even vision-language-based methods.

Act [74] and AppAgent [64] identify all interactive elements using HTML or XML data. They then assign each interactive element a unique identifier in the screenshot before feeding the screenshot into the model.

These language-based and vision-language-based methods, which rely on hierarchical information, exhibit several limitations: (1) Hierarchical representations, such as HTML or XML, are not consistently available across different platforms. And even this information is available, differences in their internal rules make language-based GUI agents less compatible; (2) HTML often contains redundant and customized information, requiring additional models or extensive manually crafted rules for effective filtering. (3) Text-based GUI agents are susceptible to injection attacks [34, 61, 71], where malicious instructions hidden in HTML can easily lead to erroneous or unsafe actions.

## 2.2. Vision-based GUI Agent

Recently, some vision-based approaches have been proposed to overcome the drawbacks of language-based methods. Some of them [2, 11, 19, 50] are single-stage methods that only use GUI screenshots as input for VLMs and output the next action in an end-to-end manner. However, these agents perform worse on GUI benchmarks compared to other methods. Two primary reasons may be the relatively low input resolution of their base models and the insufficient scale and quality of the training dataset. SeeAct [74], MobileAgent [56] and MobileAgent-v2 [55] are two-stage methods. They use GPT-4V instead of open-source VLMs as base models and find that even the top models struggle with element grounding. Consequently, they introduce additional

tools such as OCR and icon recognition models to assist with element grounding, which may increase the complexity and inference latency of the agent system. Overall, the current VLMs exhibit limited ability in handling GUI grounding tasks, thus constrains the navigation capabilities of single-stage vision-based GUI agents. We discuss additional related works on LLMs and VLMs in App. A.

## 3. Data Collection

In this section, we present a cost-effective data collection strategy designed to construct a multi-level, large-scale and high-quality GUI dataset, called **GUI-Lasagne**, as shown in Fig. 4. This dataset helps equip our models with robust abilities in GUI understanding, grounding, and navigation. The statistics of GUI-Lasagne are shown in Tab. 6.

### 3.1. Level One: Visual-Text Alignment

Visual-text alignment refers to the foundational ability of a GUI agent to perceive the visual appearance of the GUI, specifically the ability to recognize or locate text/icon elements. We collect visual-text data directly from the GUI source data. In the web scenario, we obtain website URLs from CommonCrawl [16] and website ranking sources. We then develop a data collection tool using Playwright<sup>1</sup> to gather real-world web data from the collected URLs. With this tool, we collect 755K web-page screenshots along with their DOM data, featuring diversity in both resolution and language. Additionally, we develop an icon recognition model called InternVL-Icon as an icon annotation tool, by

<sup>1</sup><https://playwright.dev/>

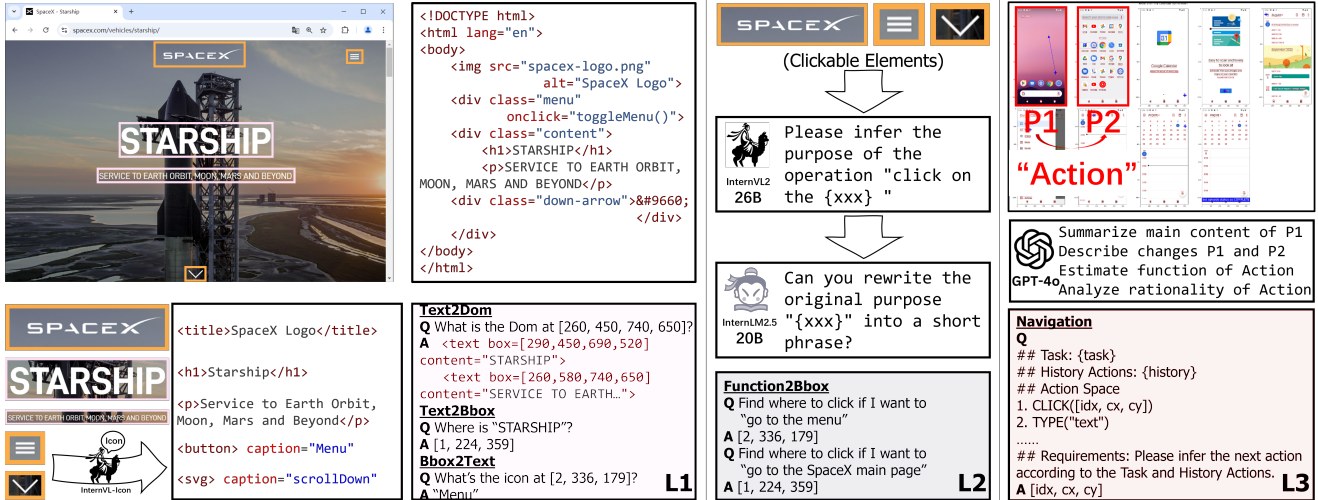


Figure 4. The collection pipeline of our GUIAsagne dataset. The left, middle and right parts show the construction of level-1, level-2, and level-3 data, respectively.

constructing a dataset of 30K icon-caption pairs from Alibaba Icon Library<sup>2</sup> and fine-tuning InternVL1.5-26B using this dataset. We then use InternVL-Icon to annotate all icons on web-pages with generated captions. As for the mobile scenario, we collect data from AitW [46], a large-scale GUI dataset on the mobile platform. See App. E.1 for more collection details.

Inspired by Lee et al. [27] and Cheng et al. [11], we construct three tasks based the collected GUI source data: text2bbox, bbox2text, and bbox2dom. The **text2bbox** task prompts the model to ground the element based on the given text or icon caption. To avoid ambiguity, we provide additional contextual information for elements that appear multiple times in the screenshots. The text2bbox data is the most abundant among the three tasks, to help the model develop robust grounding capabilities. The **bbox2text** task is the inverse of the text2bbox task, training the model to recognize text and icons. The **bbox2dom** task asks the model to generate a DOM-tree corresponding to the given bounding box, as show in App. D.4. This task helps the model learn not only to recognize text/icon elements but also to understand the GUI layout. To make sufficient use of the context length of the model, we pack multiple data pairs in each training sample for text2bbox and bbox2text task, and select the box that includes as many elements as possible for bbox2dom task. Overall, we construct a total of **1.9M** and **1.1M** training samples for the web and mobile scenarios, respectively. The data significantly enhance the GUI foundational abilities, especially the GUI grounding ability, of our SpiritSight agent. See App. F for more details on sample construction.

<sup>2</sup><https://www.iconfont.cn/?v=20230914>

### 3.2. Level two: Visual-Function Alignment

Visual-function alignment refers to a model’s ability to locate an element based on its function. This type of data is not directly accessible from the raw GUI data. Inspired by the back-translation method [48] for dataset collection in translation tasks, we leverage InternVL’s image understanding capabilities to collect function grounding data. Specifically, we divide each screenshot into a 3x3 grid and describe the approximate location of the target element in text (e.g. in the top-left corner of the image). Additionally, we place a bounding box around the target element in the screenshot to specify its precise location. We provide InternVL2-26B with the screenshot, the element’s text content or icon caption, and the location description to prompt it to generate the element’s function. Additionally, we utilize InternLM2.5-20B to enhance the quality and diversity of the generated function descriptions. These function descriptions achieve an approximate 90.9% acceptance rate based on human judgment, which we consider sufficient for constructing the function grounding pre-training data. See App. E.2 for more details on data collection and validation.

Based on the strategy above, we collect **function2bbox** pairs for all interactive elements in the web scenario. In the mobile scenario, we construct the function grounding data from the GUI navigation dataset, which is be described in Sec. 3.3. We use the same packing method as in the text2bbox and bbox2text tasks for efficient training, ultimately obtaining **1.5M** training samples.

### 3.3. Level three: Visual GUI Navigation

We utilize the public available AitW [46] dataset to construct our GUI navigation training data. AitW is a large-

scale mobile navigation dataset where each screenshot is labeled with the corresponding goal, the current step, *etc.* However, as noted in AitZ [72] and AMEX [5], the AitW dataset contains a number of incorrectly labeled samples. We choose to clean it with GPT-4o and employ Chain-of-Thought (CoT) [60] to make the judgment more accurate. Specifically, we prompt GPT-4o with the task description, the current action annotation, and screenshots from both the current and next steps. GPT-4o is then instructed to first summarize the two screenshots and identify the differences between them, then describe the current step based on these differences, and finally assess reasonability of the current action annotation. See App. E.3 for more details on data cleaning and quality verification.

We filter out steps identified as unreasonable by GPT-4o, resulting a final dataset of **0.64M** CoT-style GUI navigation training samples. With the collected CoT-style data, we are able to construct additional function grounding data for the mobile scenario, as mentioned in Sec. 3.2, by treating the collected step descriptions as functions of the corresponding elements.

### 3.4. Other Training Data

To enhance the model’s understanding of GUI content, we further collected some public datasets as a supplement, including doc/web/mobile VQA [7, 8, 20, 40], image captioning [12, 54], and mobile grounding datasets [12, 33], resulting in **0.59M** QA pairs for model training.

## 4. Universal Block Parsing

### 4.1. Problem Statement

We use InternVL2 [9] as the base model of SpiritSight, which uses a dynamic high-resolution training approach to largely preserves the details of input images. The approach first match the optimal aspect ratio from a pre-defined set of aspect ratios to each input image, then resize and divide each image into blocks of 448×448 pixels.

However, this approach may introduce ambiguity in grounding GUI elements. A typical example is represented in Fig. 5a, with two screenshots having aspect ratios of 1:2 and 2:1, respectively. According to the dynamic high-resolution strategy, the screenshots are divided into two blocks, one vertically and the other horizontally. Suppose the target elements in each sample are located in the same relative position within the second block (block-1) after cropping. The cropped screenshots are then fed into InternVL and the model is expected to predict different locations from these two identical inputs. We refer to this situation as the locational ambiguity problem.

Generally, a point  $\mathbf{p}$  is expressed in the global coordinate system as

$$\mathbf{p} = [x, y] \quad (1)$$

where  $x$  and  $y$  represent the horizontal and vertical coordinate values of the point in the original image, respectively. Assume that the image is resized and divided into  $n_w \times n_h$  blocks. We can express the point  $\mathbf{p}$  in the corresponding block as  $\mathbf{p}'$ :

$$\begin{cases} b_x = \lfloor \frac{x}{w_{block}} \rfloor \\ b_y = \lfloor \frac{y}{h_{block}} \rfloor \end{cases} \quad \begin{cases} x' = x \bmod w_{block} \\ y' = y \bmod h_{block} \end{cases} \quad (2)$$

$$\mathbf{p}' = [b_x, b_y, x', y'] \quad (3)$$

where  $w_{block}$  and  $h_{block}$  (both set to 448 in our experiments) represent the width and height of each block, respectively.  $b_x$  and  $b_y$  represent the horizontal and vertical indices of the block containing  $\mathbf{p}'$ , and  $x'$  and  $y'$  represent the coordinates of  $\mathbf{p}'$  within this block. The blocks are flattened into a sequence before being fed into the model, thus we have

$$\mathbf{p}'' = [b_i, x', y'] \quad (4)$$

where  $b_i$  represents the index of the block within the sequence, satisfying:

$$b_i = b_y \cdot n_w + b_x \quad (5)$$

The model is trained to approximate a mapping  $f : \mathbf{p}'' \rightarrow \mathbf{p}$ , which is inherently a multi-valued function. For example, when the input  $\mathbf{p}''$  is  $[1, 168, 245]$ , possible values for  $p$  include  $[168, 693]$  when  $n_w = 1$ , or  $[616, 245]$  when  $n_w = 2$ , as shown in Fig. 5a.

### 4.2. Method

The ambiguity primarily arises from the flattening operation, as shown in Eq. (5), which results in the loss of the spatial relationship between blocks. One solution is to input an additional thumbnail, but this may lead to extra computational and memory overhead. We propose to solve this positional ambiguity with two steps. Firstly, we introduce a 2D Block-wise Position Embedding (2D-BPE) [67] by adding two position embeddings to each block to capture spatial information. Secondly, we introduce a **Universal Block Parsing (UBP)** method, which replaces the global coordinate representation with a block-specific coordinate representation. Specifically, we express a point as Eq. (4). In this case, the model is trained to approximate an injective mapping  $f : \mathbf{p}'' \rightarrow \mathbf{p}$ , thereby resolving the ambiguity problem. During the model inference, the global coordinate of this point can be computed in post-processing as follows:

$$\begin{cases} x = x' + (b_i \bmod n_w) \cdot w_{block} \\ y = y' + \lfloor \frac{b_i}{n_w} \rfloor \cdot h_{block} \end{cases} \quad (6)$$

Overall, our UBP method ensures a clear mapping of positional information between the model’s inputs and outputs, thereby improving the model’s grounding capability.

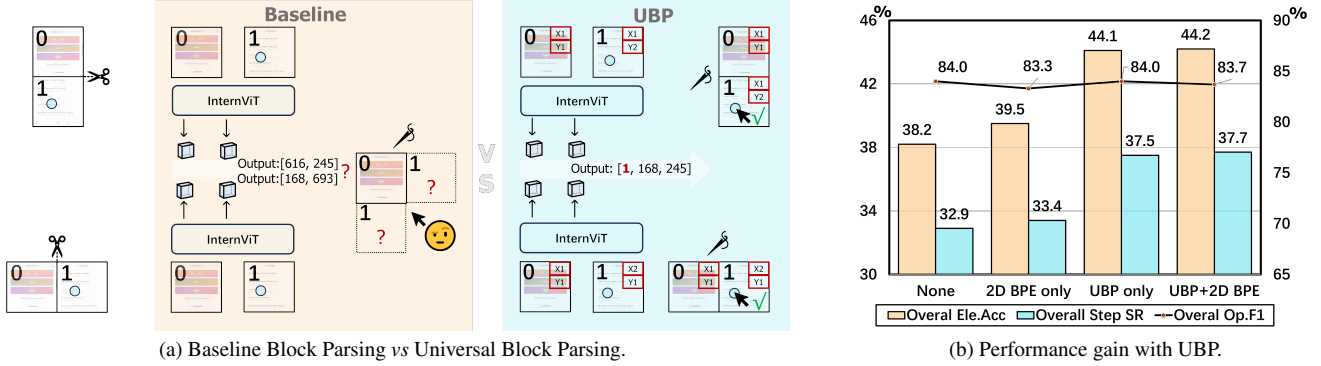


Figure 5. (a) Comparison between baseline block parsing and our proposed UBP. (b) The results of baseline block parsing and our proposed UBP methods on Multimodal-Mind2Web benchmark. UBP improves the performance of our model. The combination of UBP and 2D-BPE achieves the best results.

## 5. Settings

### 5.1. Implementation Details

We use InternVL2 (2B, 8B and 26B) [9] as the base models and train them with two stages: continual pre-training and fine-tuning. During the pre-training stage, we use all the GUI-Lasagne dataset mentioned in Sec. 3. Different prompts are designed for different training tasks to avoid task confusion. See App. F for the prompts. We unfreeze the vision encoder, decoder, and MLP layer of InternVL. The learning rate is set to  $1e-4/1e-4/5e-5$  for InternVL-2B/8B/26B, respectively, and the batch size is set to 1024. We get **SpiritSight-Base** model after pre-training and then fine-tune it on multiple downstream tasks individually. More details are shown in App. D.1 and App. D.2.

### 5.2. Benchmarks & Metrics

To assess SpiritSight’s capability in diverse real-world environments, we evaluate SpiritSight on six benchmarks covering various GUI platforms and tasks. Multimodal-Mind2Web [13], ScreenSpot [11], AMEX [5], GUIAct [7], AndroidControl [32], and GUI-Odyssey [38]. For Multimodal-Mind2Web and ScreenSpot, we use the same data pre-processing and metrics as SeeClick [11] uses. For GUIAct, we evaluate SpiritSight on the web-single and web-multi sub-sets and report step success rate (Step SR). For AndroidControl, we evaluate SpiritSight on the High-Level (HL) and Low-Level (LL) tasks and report step accuracy. For AMEX and GUI-Odyssey, we report the action matching score (AMS) defined in AitW [46]. These metrics are similar in that they all measure the single-step accuracy. Refer to App. D.3 for more information about the metrics.

## 6. Experiment

### 6.1. Advanced Vision-based GUI Agent

In this section, we compare the performance of SpiritSight with other advanced methods across various input modalities and test configurations on Multimodal-Mind2Web [13], a classic and high-quality benchmark for GUI navigation. The results are shown in Tab. 1. Methods that use top-50 candidates as input perform the best. This is evident, as the assistance of candidate elements can significantly reduce the decision space. However, such methods are not particularly feasible in practice.

The results indicate that SpiritSight significantly outperforms all methods that do not rely on any candidate element, including vision-based methods, language-based methods, and even vision-language-based methods. This demonstrates strong capabilities of SpiritSight in Web GUI navigation tasks. It should be noted that SpiritSight achieves a significant advantage in the Ele.Acc metric compared to other vision-based methods, which can be attributed to the specially constructed visual grounding training data and the proposed UBP approach.

### 6.2. Strong Cross-Platform Compatibility

We evaluated SpiritSight on other GUI navigation benchmarks across various platforms and compare it with state-of-the-art (SOTA) GUI agents as shown in Tab. 2. SpiritSight demonstrated the best performance on these benchmarks, showing its strong capabilities across various platforms. OdysseyAgent uses additional historical screenshot images as input, yet SpiritSight achieves comparable results.

We also evaluated SpiritSight on ScreenSpot, a function grounding benchmark. As shown in Tab. 3, SpiritSight performs well across all three platforms, showcasing its cross-platform capability and robust grounding ability. Notably, SpiritSight models are trained specifically for GUI naviga-

Agent	Odyssey AMEX		AndroidCtrl		GUIAct	
	High	High	High	Low	Multi	Single
GPT-4o[42]	20.4%	-	21.2%	28.4%	-	41.8%
Previous SOTA	74.3%	70.7%	64.8%	80.0%	45.4%	74.9%
SpiritSight-2B	72.3%	74.5%	64.9%	86.3%	45.5%	76.0%
SpiritSight-8B	<b>75.8%</b>	<b>80.7%</b>	<b>68.1%</b>	<b>87.6%</b>	<b>49.3%</b>	<b>78.2%</b>

Table 2. Results of SpiritSight on four recently published GUI navigation benchmarks. 'High' and 'Multi' indicates high-level tasks, 'Low' and 'Single' indicates single-stepped tasks. The SOTA results of GUI-Odyssey, AMEX, AndroidControl and GUIAct come from OdysseyAgent [38], SPHINX-GUI-Agent [5], fine-tuned PaLM-2S [32] and MiniCPM-GUI [7], respectively.

tion tasks, with no training data intentionally aligning with ScreenSpot is collected. There remains room for further improvement in SpiritSight’s performance on the ScreenSpot benchmark. We further assess the foundational ability of SpiritSight, the visual grounding ability, on our custom-constructed testing dataset. See App. D.4 for more details.

### 6.3. Recognition and Grounding as Priors for GUI Navigation

To verify the significance of the three levels of GUI-Lasagne data, we progressively removed level-3, level-2, and level-1 data from the training set during the pre-training stage and evaluate SpiritSight-8B on Multimodal-Mind2Web. The results are shown by the blue line in Fig. 6a. It can be seen that each level of data contributes to improving Step SR. While the tasks in level-1 data differ the most from web navigation task compared to the other two levels, they provide an effective initialization for the pre-trained model. Although the level-3 data is constructed from the mobile scenario, it also assists in web-based GUI navigation tasks. This indicates that the joint learning strategy helps SpiritSight develop strong navigation abilities across different GUI environments with limited resources.

We also conducted ablation experiments to evaluate the effectiveness of data cleaning and CoT construction strategies on the level-3 data, as shown by the orange line in Fig. 6a. It can be observed that training in a CoT manner effectively improve the model’s GUI navigation capabilities, while the impact of data cleaning strategy is relatively small. This may be due to the fact that erroneous samples are relatively tolerated during the pre-training phase of large models. The difference in results of "w/ CoT" and "w/ Level 1+2+3" is due to the different implementation for fine-tuning stage. See App. D.2 for more details.

To evaluate the effectiveness of our GUI-Lasagne dataset, we train InternVL-2 (8B) on SeeClick training data [11] using full parameter training and LoRA training, resulting

Agent	Model Size	ScreenSpot		
		Web	Mobile	Desktop
GPT4V[1]	-	5.0%	7.5%	4.6%
Qwen-VL[3]	9.6B	3.0%	7.2%	5.4%
Fuyu[4]	8B	19.2%	21.2%	18.3%
CogAgent[19]	18B	49.5%	45.5%	47.1%
SeeClick[11]	9.6B	44.1%	65.0%	51.1%
SpiritSight-2B	2B	63.6%	62.5%	61.8%
SpiritSight-8B	8B	<b>68.3%</b>	<b>68.4%</b>	<b>62.9%</b>

Table 3. Results of SpiritSight and other vision-based methods on ScreenSpot Benchmark.

in SeeClick(InternVL-Full) and SeeClick(InternVL-LoRA), respectively. We then fine-tune and evaluate the two models on the Multimodal-Mind2Web benchmark. The results are shown by the dashed line in Fig. 6a, where we also present the result of the original SeeClick model. SeeClick(InternVL-LoRA) performs better than the original SeeClick model, which may be attributed to the dynamic high-resolution approach used by InternVL that preserves the details of input images. SeeClick(InternVL-Full) performs the worst, as the scale of the SeeClick training data is not large enough for the model to converge during full parameter training. SpiritSight agent that trained on only GUI-Lasagne level-1 data outperforms all three models trained on SeeClick data, demonstrating the effectiveness of GUI-Lasagne dataset.

### 6.4. Better Grounding Ability from UBP

To verify the effectiveness of UBP on grounding task, we use LoRA for resource efficiency to fine-tune InternVL in 4 different settings (original as baseline, 2D-BPE, UBP, and 2D-BPE&UBP), respectively. We then evaluate these models on Multimodal-Mind2Web benchmark, as shown in Fig. 5b. It can be seen that UBP shows a significant advantage in Ele.Acc compared to baseline, while the results of Op.F1 show little variation across the 4 settings. This indicates that UBP improves the performance of GUI agent primarily by enhancing the grounding ability. Finally, the combination of UBP and 2D-BPE achieves the best results. This indicates that UBP is compatible with 2D-BPE, leading to better performance.

### 6.5. Scaling Effects on Dataset and Model Size

We explore the impact of pre-training dataset and model size on SpiritSight using Multimodal-Mind2Web benchmark. The results are shown in Fig. 6b. SpiritSight-2B outperforms SeeClick [11] by using just 1/8 of the pre-training dataset. This impressive performance comes from the high quality and grounding-focus nature of GUI-Lasagne data.

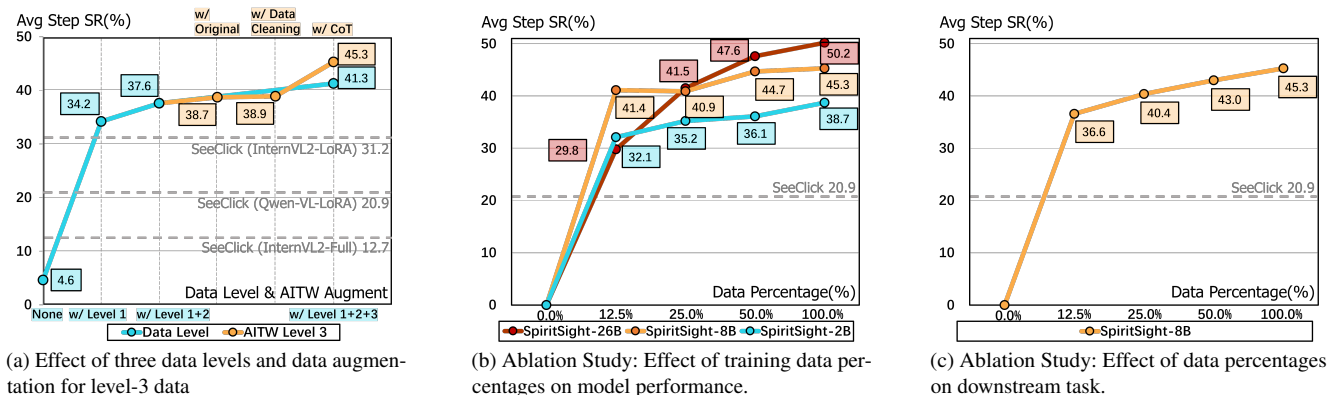


Figure 6. Ablation studies on GUILasagne dataset and scaling effects in the Multimodal-Mind2Web benchmark.

The performance improves as the size of dataset increases, demonstrating the significance of collecting large-scale data. SpiritSight-2B reaches saturation with a smaller amount of pre-training data, while SpiritSight-26B appears to have further potential for improvement, which aligns with the scaling law of LLMs and VLMs.

We also evaluate the ability of SpiritSight to transferring to downstream GUI agent tasks. We fine-tune SpiritSight-Base (8B) on various proportions of the Multimodal-Mind2Web training data and show the results in Fig. 6c. It is noticed that SpiritSight achieves 36.6% Step SR with only 1/8 of the fine-tuning data, showing strong transferability to GUI navigation tasks.

## 6.6. Effective Transfer to other languages

Exploring the cross-lingual capabilities of GUI agents is highly beneficial for their application in non-English environments. We split the training and testing sets of GUIAct (web-multi) dataset into English and Chinese partitions, respectively. We then fine-tune SpiritSight-Base (8B) on two sets of data: the entire training set (English&Chinese) and the English-only training set. The results are shown in Tab. 4.

Under the English&Chinese configuration, SpiritSight achieves comparable results on both the English and Chinese testing sets, despite having fewer Chinese samples in the pre-training dataset than English ones. Under the English-only configuration, SpiritSight achieves 24.5% Step SR on the Chinese testing set, reaching half of the English&Chinese performance. The zero-shot capability of SpiritSight in Chinese results from the small but effective foundational Chinese data included in the pre-training stage.

This experiment offers a paradigm for applying GUI agents to non-English environments: by collecting (1) free web and mobile GUI information from the target language environment (level 1 & level 2 data), and (2) a small amount of high-quality GUI navigation data at low cost (level 3 data). With this language transferring strategy, the same ca-

SFT Data	Overall	Chinese	English
English+Chinese	49.3%	49.3%	49.2%
English	35.0%	24.5%	48.6%

Table 4. Results of SpiritSight on GUIAct (web-multi), trained with different language datasets.

pabilities as in the English environment can be achieved in non-English environments with minimal extra costs.

## 7. Limitation

As SpiritSight is a vision-based GUI agent, it constantly requires access to screenshots which may contain personal information or other sensitive data. Users and system providers should carefully manage the system privileges granted to SpiritSight agent to mitigate potential privacy and security risks.

## 8. Conclusion

In this paper, we propose an advanced vision-based end-to-end GUI agent, SpiritSight, with high generalization across multiple GUI platforms. We construct an efficient multi-level, large-scale, high-quality GUI pre-training dataset to equip SpiritSight with robust GUI perception, grounding and understanding capabilities. Additionally, we introduce a UBP method to resolve ambiguity in dynamic high-resolution inputs during model training, further enhancing the ability of SpiritSight to ground GUI objects. As a result, SpiritSight achieves strong performance in numerous GUI navigation benchmarks, demonstrating significant potential for practical deployment in real-world applications.



## References

- [1] Josh Achiam, Steven Adler, Sandhini Agarwal, Lama Ahmad, Ilge Akkaya, Florencia Leoni Aleman, Diogo Almeida, Janko Altenschmidt, Sam Altman, Shyamal Anadkat, et al. Gpt-4 technical report. *arXiv preprint arXiv:2303.08774*, 2023. 7
- [2] Gilles Baechler, Srinivas Sunkara, Maria Wang, Fedir Zubach, Hassan Mansoor, Vincent Etter, Victor Cărbune, Jason Lin, Jindong Chen, and Abhanshu Sharma. Screenai: A vision-language model for ui and infographics understanding. *arXiv preprint arXiv:2402.04615*, 2024. 3
- [3] Jinze Bai, Shuai Bai, Shusheng Yang, Shijie Wang, Sinan Tan, Peng Wang, Junyang Lin, Chang Zhou, and Jingren Zhou. Qwen-vl: A frontier large vision-language model with versatile abilities. *arXiv preprint arXiv:2308.12966*, 2023. 7, 12
- [4] Rohan Bavishi, Erich Elsen, Curtis Hawthorne, Maxwell Nye, Augustus Odena, Arushi Somani, and Saġnak Taşırlar. Introducing our multimodal models, 2023. 3, 7
- [5] Yuxiang Chai, Siyuan Huang, Yazhe Niu, Han Xiao, Liang Liu, Dingyu Zhang, Peng Gao, Shuai Ren, and Hongsheng Li. Amex: Android multi-annotation expo dataset for mobile gui agents. *arXiv preprint arXiv:2407.17490*, 2024. 2, 5, 6, 7, 12, 15, 17
- [6] Dongping Chen, Yue Huang, Siyuan Wu, Jingyu Tang, Liuyi Chen, Yilin Bai, Zhigang He, Chenlong Wang, Huichi Zhou, Yiqiang Li, et al. Gui-world: A dataset for gui-oriented multimodal llm-based agents. *arXiv preprint arXiv:2406.10819*, 2024. 2
- [7] Wentong Chen, Junbo Cui, Jinyi Hu, Yujia Qin, Junjie Fang, Yue Zhao, Chongyi Wang, Jun Liu, Guirong Chen, Yupeng Huo, et al. Guicourse: From general vision language models to versatile gui agents. *arXiv preprint arXiv:2406.11317*, 2024. 1, 3, 5, 6, 7, 12, 15
- [8] Xingyu Chen, Zihan Zhao, Lu Chen, Danyang Zhang, Jiabao Ji, Ao Luo, Yuxuan Xiong, and Kai Yu. Websrc: A dataset for web-based structural reading comprehension. *arXiv preprint arXiv:2101.09465*, 2021. 5
- [9] Zhe Chen, Weiyun Wang, Hao Tian, Shenglong Ye, Zhangwei Gao, Erfei Cui, Wenwen Tong, Kongzhi Hu, Jiapeng Luo, Zheng Ma, et al. How far are we to gpt-4v? closing the gap to commercial multimodal models with open-source suites. *arXiv preprint arXiv:2404.16821*, 2024. 2, 5, 6, 12, 13
- [10] Zhe Chen, Jiannan Wu, Wenhai Wang, Weijie Su, Guo Chen, Sen Xing, Muyan Zhong, Qinglong Zhang, Xizhou Zhu, Lewei Lu, et al. Internvl: Scaling up vision foundation models and aligning for generic visual-linguistic tasks. In *Proceedings of the IEEE/CVF Conference on Computer Vision and Pattern Recognition*, pages 24185–24198, 2024. 12
- [11] Kanzhi Cheng, Qiushi Sun, Yougang Chu, Fangzhi Xu, Yantao Li, Jianbing Zhang, and Zhiyong Wu. Seeclick: Harnessing gui grounding for advanced visual gui agents. *arXiv preprint arXiv:2401.10935*, 2024. 1, 3, 4, 6, 7, 12, 13, 15
- [12] Biplab Deka, Zifeng Huang, Chad Franzen, Joshua Hibschman, Daniel Afegan, Yang Li, Jeffrey Nichols, and Ranjitha Kumar. Rico: A mobile app dataset for building data-driven design applications. In *Proceedings of the 30th annual ACM symposium on user interface software and technology*, pages 845–854, 2017. 5, 13
- [13] Xiang Deng, Yu Gu, Boyuan Zheng, Shijie Chen, Sam Stevens, Boshi Wang, Huan Sun, and Yu Su. Mind2web: Towards a generalist agent for the web. *Advances in Neural Information Processing Systems*, 36, 2024. 1, 2, 6, 12, 15
- [14] Jacob Devlin. Bert: Pre-training of deep bidirectional transformers for language understanding. *arXiv preprint arXiv:1810.04805*, 2018. 12
- [15] Hiroki Furuta, Kuang-Huei Lee, Ofir Nachum, Yutaka Matsuo, Aleksandra Faust, Shixiang Shane Gu, and Izzeddin Gur. Multimodal web navigation with instruction-finetuned foundation models. *arXiv preprint arXiv:2305.11854*, 2023. 1, 2
- [16] Common Crawl Group. Common crawl - open repository of web crawl data, 2024. 3, 15
- [17] Izzeddin Gur, Hiroki Furuta, Austin Huang, Mustafa Safdari, Yutaka Matsuo, Douglas Eck, and Aleksandra Faust. A real-world webagent with planning, long context understanding, and program synthesis. *arXiv preprint arXiv:2307.12856*, 2023. 2, 3
- [18] Markus Hafner, Maria Katsantoni, Tino Köster, James Marks, Joyita Mukherjee, Dorothee Staiger, Jernej Ule, and Mihaela Zavolan. Clip and complementary methods. *Nature Reviews Methods Primers*, 1(1):1–23, 2021. 12
- [19] Wenyi Hong, Weihang Wang, Qingsong Lv, Jiazheng Xu, Wenmeng Yu, Junhui Ji, Yan Wang, Zihan Wang, Yuxiao Dong, Ming Ding, et al. Cogagent: A visual language model for gui agents. In *Proceedings of the IEEE/CVF Conference on Computer Vision and Pattern Recognition*, pages 14281–14290, 2024. 1, 3, 7
- [20] Yu-Chung Hsiao, Fedir Zubach, Maria Wang, et al. Screenqa: Large-scale question-answer pairs over mobile app screenshots. *arXiv preprint arXiv:2209.08199*, 2022. 5
- [21] Edward J Hu, Yelong Shen, Phillip Wallis, Zeyuan Allen-Zhu, Yuanzhi Li, Shean Wang, Lu Wang, and Weizhu Chen. Lora: Low-rank adaptation of large language models. *arXiv preprint arXiv:2106.09685*, 2021. 13
- [22] Faria Huq, Jeffrey P Bigham, and Nikolas Martelaro. "what's important here?": Opportunities and challenges of using llms in retrieving information from web interfaces. *arXiv preprint arXiv:2312.06147*, 2023. 1
- [23] Yang Jin, Kun Xu, Kun Xu, Liwei Chen, Chao Liao, Jianchao Tan, Quzhe Huang, Bin Chen, Chenyi Lei, An Liu, et al. Unified language-vision pretraining in llm with dynamic discrete visual tokenization. arxiv 2024. *arXiv preprint arXiv:2309.04669*, 2023. 12
- [24] Jihyung Kil, Chan Hee Song, Boyuan Zheng, Xiang Deng, Yu Su, and Wei-Lun Chao. Dual-view visual contextualization for web navigation. In *Proceedings of the IEEE/CVF Conference on Computer Vision and Pattern Recognition*, pages 14445–14454, 2024. 1
- [25] Geewook Kim, Teakgyu Hong, Moonbin Yim, JeongYeon Nam, Jinyoung Park, Jinyeong Yim, Wonseok Hwang, Sangdoo Yun, Dongyoon Han, and Seunghyun Park. Ocr-free document understanding transformer. In *European Conference on Computer Vision*, pages 498–517. Springer, 2022. 12, 13

- [26] Hanyu Lai, Xiao Liu, Iat Long Iong, Shuntian Yao, Yuxuan Chen, Pengbo Shen, Hao Yu, Hanchen Zhang, Xiaohan Zhang, Yuxiao Dong, et al. Autowebglm: Bootstrap and reinforce a large language model-based web navigating agent. *arXiv preprint arXiv:2404.03648*, 2024. 1, 2, 3
- [27] Kenton Lee, Mandar Joshi, Iulia Raluca Turc, Hexiang Hu, Fangyu Liu, Julian Martin Eisenschlos, Urvashi Khandelwal, Peter Shaw, Ming-Wei Chang, and Kristina Toutanova. Pix2struct: Screenshot parsing as pretraining for visual language understanding. In *International Conference on Machine Learning*, pages 18893–18912. PMLR, 2023. 2, 4
- [28] Kuang-Huei Lee, Xinyun Chen, Hiroki Furuta, John Canny, and Ian Fischer. A human-inspired reading agent with gist memory of very long contexts. *arXiv preprint arXiv:2402.09727*, 2024. 1, 3
- [29] Feng Li, Renrui Zhang, Hao Zhang, Yuanhan Zhang, Bo Li, Wei Li, Zejun Ma, and Chunyuan Li. Llava-next-interleave: Tackling multi-image, video, and 3d in large multimodal models. *arXiv preprint arXiv:2407.07895*, 2024. 12
- [30] Junnan Li, Dongxu Li, Caiming Xiong, and Steven Hoi. Blip: Bootstrapping language-image pre-training for unified vision-language understanding and generation. In *International conference on machine learning*, pages 12888–12900. PMLR, 2022. 12
- [31] Junnan Li, Dongxu Li, Silvio Savarese, and Steven Hoi. Blip-2: Bootstrapping language-image pre-training with frozen image encoders and large language models. In *International conference on machine learning*, pages 19730–19742. PMLR, 2023. 12
- [32] Wei Li, William Bishop, Alice Li, Chris Rawles, Folawiyo Campbell-Ajala, Divya Tyamagundlu, and Oriana Riva. On the effects of data scale on computer control agents. *arXiv preprint arXiv:2406.03679*, 2024. 6, 7, 12, 15
- [33] Yang Li, Gang Li, Luheng He, Jingjie Zheng, Hong Li, and Zhiwei Guan. Widget-captioning: Generating natural language description for mobile user interface elements. *arXiv preprint arXiv:2010.04295*, 2020. 5, 13
- [34] Zeyi Liao, Lingbo Mo, Chejian Xu, Mintong Kang, Jiawei Zhang, Chaowei Xiao, Yuan Tian, Bo Li, and Huan Sun. Eia: Environmental injection attack on generalist web agents for privacy leakage. *arXiv preprint arXiv:2409.11295*, 2024. 1, 3
- [35] Ziyi Lin, Chris Liu, Renrui Zhang, Peng Gao, Longtian Qiu, Han Xiao, Han Qiu, Chen Lin, Wenqi Shao, Keqin Chen, et al. Sphinx: The joint mixing of weights, tasks, and visual embeddings for multi-modal large language models. *arXiv preprint arXiv:2311.07575*, 2023. 12
- [36] Evan Zheran Liu, Kelvin Guu, Panupong Pasupat, Tianlin Shi, and Percy Liang. Reinforcement learning on web interfaces using workflow-guided exploration. *arXiv preprint arXiv:1802.08802*, 2018. 2, 12
- [37] Haotian Liu, Chunyuan Li, Qingyang Wu, and Yong Jae Lee. Visual instruction tuning, 2023. 12
- [38] Quanfeng Lu, Wenqi Shao, Zitao Liu, Fanqing Meng, Boxuan Li, Botong Chen, Siyuan Huang, Kaipeng Zhang, Yu Qiao, and Ping Luo. Gui odyssey: A comprehensive dataset for cross-app gui navigation on mobile devices. *arXiv preprint arXiv:2406.08451*, 2024. 2, 6, 7, 12, 15
- [39] Xing Han Lù, Zdeněk Kasner, and Siva Reddy. Weblinx: Real-world website navigation with multi-turn dialogue. *arXiv preprint arXiv:2402.05930*, 2024. 2
- [40] Minesh Mathew, Dimosthenis Karatzas, and CV Jawahar. Docvqa: A dataset for vqa on document images. In *Proceedings of the IEEE/CVF winter conference on applications of computer vision*, pages 2200–2209, 2021. 5
- [41] Erik Nijkamp, Bo Pang, Hiroaki Hayashi, Lifu Tu, Huan Wang, Yingbo Zhou, Silvio Savarese, and Caiming Xiong. Codegen: An open large language model for code with multi-turn program synthesis. *arXiv preprint arXiv:2203.13474*, 2022. 12
- [42] OpenAI. Hello gpt-4o, 2024. 7
- [43] Liangming Pan, Alon Albalak, Xinyi Wang, and William Yang Wang. Logic-lm: Empowering large language models with symbolic solvers for faithful logical reasoning. *arXiv preprint arXiv:2305.12295*, 2023. 12
- [44] Alec Radford, Karthik Narasimhan, Tim Salimans, Ilya Sutskever, et al. Improving language understanding by generative pre-training. *OpenAI*, 2018.
- [45] Colin Raffel, Noam Shazeer, Adam Roberts, Katherine Lee, Sharan Narang, Michael Matena, Yanqi Zhou, Wei Li, and Peter J Liu. Exploring the limits of transfer learning with a unified text-to-text transformer. *Journal of machine learning research*, 21(140):1–67, 2020. 12
- [46] Christopher Rawles, Alice Li, Daniel Rodriguez, Oriana Riva, and Timothy Lillicrap. Androidinthewild: A large-scale dataset for android device control. *Advances in Neural Information Processing Systems*, 36, 2024. 2, 4, 6, 12, 17
- [47] Baptiste Roziere, Jonas Gehring, Fabian Gloeckle, Sten Sootla, Itai Gat, Xiaoqing Ellen Tan, Yossi Adi, Jingyu Liu, Romain Sauvestre, Tal Remez, et al. Code llama: Open foundation models for code. *arXiv preprint arXiv:2308.12950*, 2023. 12
- [48] Rico Sennrich. Improving neural machine translation models with monolingual data. *arXiv preprint arXiv:1511.06709*, 2015. 4
- [49] Zhihong Shao, Peiyi Wang, Qihao Zhu, Runxin Xu, Junxiao Song, Mingchuan Zhang, YK Li, Yu Wu, and Daya Guo. Deepseekmath: Pushing the limits of mathematical reasoning in open language models. *arXiv preprint arXiv:2402.03300*, 2024. 12
- [50] Peter Shaw, Mandar Joshi, James Cohan, Jonathan Berant, Panupong Pasupat, Hexiang Hu, Urvashi Khandelwal, Kenton Lee, and Kristina N Toutanova. From pixels to ui actions: Learning to follow instructions via graphical user interfaces. *Advances in Neural Information Processing Systems*, 36:34354–34370, 2023. 3
- [51] Tianlin Shi, Andrej Karpathy, Linxi Fan, Jonathan Hernandez, and Percy Liang. World of bits: An open-domain platform for web-based agents. In *International Conference on Machine Learning*, pages 3135–3144. PMLR, 2017. 2, 12
- [52] Lucas-Andrei Thil, Mirela Popa, and Gerasimos Spanakis. Navigating webai: Training agents to complete web tasks with large language models and reinforcement learning. In *Proceedings of the 39th ACM/SIGAPP Symposium on Applied Computing*, pages 866–874, 2024. 1, 2

- [53] Jianqiang Wan, Sibao Song, Wenwen Yu, Yuliang Liu, Wenqing Cheng, Fei Huang, Xiang Bai, Cong Yao, and Zhibo Yang. Omniparser: A unified framework for text spotting key information extraction and table recognition. In *Proceedings of the IEEE/CVF Conference on Computer Vision and Pattern Recognition*, pages 15641–15653, 2024. 1, 3
- [54] Bryan Wang, Gang Li, Xin Zhou, Zhourong Chen, Tovi Grossman, and Yang Li. Screen2words: Automatic mobile ui summarization with multimodal learning. In *The 34th Annual ACM Symposium on User Interface Software and Technology*, pages 498–510, 2021. 5, 13
- [55] Junyang Wang, Haiyang Xu, Haitao Jia, Xi Zhang, Ming Yan, Weizhou Shen, Ji Zhang, Fei Huang, and Jitao Sang. Mobile-agent-v2: Mobile device operation assistant with effective navigation via multi-agent collaboration. *arXiv preprint arXiv:2406.01014*, 2024. 1, 3
- [56] Junyang Wang, Haiyang Xu, Jiabo Ye, Ming Yan, Weizhou Shen, Ji Zhang, Fei Huang, and Jitao Sang. Mobile-agent: Autonomous multi-modal mobile device agent with visual perception. *arXiv preprint arXiv:2401.16158*, 2024. 1, 3
- [57] Ke Wang, Houxing Ren, Aojun Zhou, Zimu Lu, Sichun Luo, Weikang Shi, Renrui Zhang, Linqi Song, Mingjie Zhan, and Hongsheng Li. Mathcoder: Seamless code integration in llms for enhanced mathematical reasoning. *arXiv preprint arXiv:2310.03731*, 2023. 12
- [58] Weihang Wang, Qingsong Lv, Wenmeng Yu, Wenyi Hong, Ji Qi, Yan Wang, Junhui Ji, Zhuoyi Yang, Lei Zhao, Xixuan Song, et al. CogVLM: Visual expert for pretrained language models. *arXiv preprint arXiv:2311.03079*, 2023. 12
- [59] Jason Wei, Yi Tay, Rishi Bommasani, Colin Raffel, Barret Zoph, Sebastian Borgeaud, Dani Yogatama, Maarten Bosma, Denny Zhou, Donald Metzler, et al. Emergent abilities of large language models. *arXiv preprint arXiv:2206.07682*, 2022. 12
- [60] Jason Wei, Xuezhi Wang, Dale Schuurmans, Maarten Bosma, Fei Xia, Ed Chi, Quoc V Le, Denny Zhou, et al. Chain-of-thought prompting elicits reasoning in large language models. *Advances in neural information processing systems*, 35:24824–24837, 2022. 5, 12, 17
- [61] Chen Henry Wu, Jing Yu Koh, Ruslan Salakhutdinov, Daniel Fried, and Aditi Raghunathan. Adversarial attacks on multimodal agents. *arXiv preprint arXiv:2406.12814*, 2024. 1, 3
- [62] Shijie Wu, Ozan Irsoy, Steven Lu, Vadim Dabravolski, Mark Dredze, Sebastian Gehrmann, Prabhajan Kambadur, David Rosenberg, and Gideon Mann. Bloomberggpt: A large language model for finance. *arXiv preprint arXiv:2303.17564*, 2023. 12
- [63] Yichong Xu, Chenguang Zhu, Shuohang Wang, Siqi Sun, Hao Cheng, Xiaodong Liu, Jianfeng Gao, Pengcheng He, Michael Zeng, and Xuedong Huang. Human parity on commonsenseqa: Augmenting self-attention with external attention. *arXiv preprint arXiv:2112.03254*, 2021. 12
- [64] Zhao Yang, Jiakuan Liu, Yucheng Han, Xin Chen, Zebiao Huang, Bin Fu, and Gang Yu. Appagent: Multimodal agents as smartphone users. *arXiv preprint arXiv:2312.13771*, 2023. 3
- [65] Shunyu Yao, Howard Chen, John Yang, and Karthik Narasimhan. Webshop: Towards scalable real-world web interaction with grounded language agents. *Advances in Neural Information Processing Systems*, 35:20744–20757, 2022. 2, 12
- [66] Yuan Yao, Tianyu Yu, Ao Zhang, Chongyi Wang, Junbo Cui, Hongji Zhu, Tianchi Cai, Haoyu Li, Weilin Zhao, Zhihui He, et al. Minicpm-v: A gpt-4v level mllm on your phone. *arXiv preprint arXiv:2408.01800*, 2024. 12
- [67] Jiabo Ye, Anwen Hu, Haiyang Xu, Qinghao Ye, Ming Yan, Guohai Xu, Chenliang Li, Junfeng Tian, Qi Qian, Ji Zhang, et al. Ureader: Universal ocr-free visually-situated language understanding with multimodal large language model. *arXiv preprint arXiv:2310.05126*, 2023. 2, 5
- [68] Da Yin, Faeze Brahman, Abhilasha Ravichander, Khyathi Chandu, Kai-Wei Chang, Yejin Choi, and Bill Yuchen Lin. Agent lumos: Unified and modular training for open-source language agents. In *Proceedings of the 62nd Annual Meeting of the Association for Computational Linguistics (Volume 1: Long Papers)*, pages 12380–12403, 2024. 1
- [69] Huaiyuan Ying, Shuo Zhang, Linyang Li, Zhejiang Zhou, Yunfan Shao, Zhaoye Fei, Yichuan Ma, Jiawei Hong, Kuikun Liu, Ziyi Wang, et al. Internlm-math: Open math large language models toward verifiable reasoning. *arXiv preprint arXiv:2402.06332*, 2024. 12
- [70] Longhui Yu, Weisen Jiang, Han Shi, Jincheng Yu, Zhengying Liu, Yu Zhang, James T Kwok, Zhenguo Li, Adrian Weller, and Weiyang Liu. Metamath: Bootstrap your own mathematical questions for large language models. *arXiv preprint arXiv:2309.12284*, 2023. 12
- [71] Qiusi Zhan, Zhixiang Liang, Zifan Ying, and Daniel Kang. Injecagent: Benchmarking indirect prompt injections in tool-integrated large language model agents. *arXiv preprint arXiv:2403.02691*, 2024. 1, 3
- [72] Jiwen Zhang, Jihao Wu, Yihua Teng, Minghui Liao, Nuo Xu, Xiao Xiao, Zhongyu Wei, and Duyu Tang. Android in the zoo: Chain-of-action-thought for gui agents. *arXiv preprint arXiv:2403.02713*, 2024. 5, 17
- [73] Pan Zhang, Xiaoyi Dong, Yuhang Zang, Yuhang Cao, Rui Qian, Lin Chen, Qipeng Guo, Haodong Duan, Bin Wang, Linke Ouyang, Songyang Zhang, Wenwei Zhang, Yining Li, Yang Gao, Peng Sun, Xinyue Zhang, Wei Li, Jingwen Li, Wenhai Wang, Hang Yan, Conghui He, Xingcheng Zhang, Kai Chen, Jifeng Dai, Yu Qiao, Dahua Lin, and Jiaqi Wang. Internlm-xcomposer-2.5: A versatile large vision language model supporting long-contextual input and output, 2024. 12
- [74] Boyuan Zheng, Boyu Gou, Jihyung Kil, Huan Sun, and Yu Su. Gpt-4v (ision) is a generalist web agent, if grounded. *arXiv preprint arXiv:2401.01614*, 2024. 1, 3
- [75] Longtao Zheng, Rundong Wang, Xinrun Wang, and Bo An. Synapse: Trajectory-as-exemplar prompting with memory for computer control. In *The Twelfth International Conference on Learning Representations*, 2023. 1

## A. Extended Related Work

### A.1. Large-scale Language Models

In recent years, large language models (LLMs) [14, 41, 43–45, 47, 49, 57, 59, 60, 62, 63, 69, 70] have demonstrated remarkable capabilities in the field of Natural Language Processing (NLP), encompassing natural language generation, commonsense knowledge question-answering, code completion, mathematical computation, and logical reasoning. LLM have also demonstrated strong decision-making capabilities, laying the foundation for the emergence of GUI agents.

### A.2. Visual Large-scale Language Models

With the development of large language models, numerous works [3, 9, 23, 29, 35, 58, 66, 73] have proposed vision language models (VLMs) to bring the capabilities of language models into the visual domain. CLIP [18] uses contrastive learning to align vision and language features, while BLIP [30] and BLIP-2 [31] build on this by adding a language decoder, enabling the models to perform image-grounded text generation. InternVL [10] attempts to scale the parameters of vision encoder up to 6 billion, significantly enhancing the model’s ability to perceive visual input. LLaVA [37] and Sphinx [35] improve the models’ understanding and chat abilities through instruction tuning and multitask learning, respectively. Beyond general domains, OCR-Free [25] methods use an encoder-decoder architecture to achieve end-to-end visual document understanding. This demonstrates the significant potential of VLMs in GUI navigation tasks.

### A.3. GUI Agent Benchmarks

GUI agents have seen rapid development in recent years, with many types of benchmarks emerging. MiniWoB [51], MiniWoB++ [36], and WebShop [65] are early classic GUI navigation benchmarks. However, the data in these benchmarks is synthetically generated, which creates a slight gap compared to real-world data. AitW [46] is a large-scale real-world dataset designed for mobile navigation tasks, and Mind2Web [13] is a high-quality benchmark for web navigation that provide evaluation across three scenario: cross-task, cross-website, and cross-domain. ScreenSpot [11] is a functional grounding benchmark that covers mobile, web, and desktop scenarios. GUIAct [7], AMEX [5], AndroidControl [32], and GUI Odyssey [38] are newly released benchmarks designed for web and mobile environments, respectively. They are highly reliable benchmarks as they are annotated by humans and have undergone further validation. In this paper, we evaluate SpiritSight on six benchmarks across different GUI platforms and tasks: MultimodalMind2Web [13], ScreenSpot [11], GUIAct [5], AMEX [5], AndroidControl [32], and GUI Odyssey [38]. Overview of these benchmarks is shown in Tab. 5

## B. Task Formulation

For a given GUI platform, we first obtain an action space  $\mathcal{A}$  that contains all operable actions. Given the task description  $\mathcal{T}$ , the previous actions  $\mathcal{H} = \{a_1, a_2, \dots, a_{t-1}\}$ , the action space  $\mathcal{A}$  and the current screenshot  $o_t$ , the agent is expected to infer the optimal action  $a_t^*$  that maximizes the expected future reward. The inference process is guided by a policy  $\pi$ , as shown below, which maps the current context to a probability distribution over the action space  $\mathcal{A}$ . Here,  $a$  denotes a specific action selected from the action space  $\mathcal{A}$ .

$$a_t^* \sim \pi(a|\mathcal{T}, \mathcal{H}, \mathcal{A}, o_t), \quad a \in \mathcal{A} \quad (7)$$

We propose a hierarchical decomposition of the policy to manage the complexity of action inference. Initially, we define  $s$  as the natural language description (*e.g.* Click on the login button.) of action  $a$  (*e.g.* CLICK(132, 243)). We decompose the overall policy  $\pi$  into a step inference policy  $\pi_s$  and an action inference policy  $\pi_a$  as Eq. (8). The step inference policy  $\pi_s$  selects the optimal  $s$  based on the current context. Once  $s$  is determined, the action inference policy  $\pi_a$  predicts the corresponding action  $a$  from the action space  $\mathcal{A}$ .

$$\pi(a|\mathcal{T}, \mathcal{H}, \mathcal{A}, o_t) = \pi_s(s|\mathcal{T}, \mathcal{H}, o_t) \cdot \pi_a(a|s, \mathcal{A}) \quad (8)$$

Further, we decompose  $\pi_a$  into  $\pi_{pos}$  and  $\pi_{attr}$  as Eq. (9). Here,  $a_{pos}$  denotes to the positional aspect of the action, typically the coordinates where the action is performed (*e.g.* (132, 243)), while  $a_{attr}$  denotes the non-positional aspects, such as the action type (*e.g.* click) or additional parameters like specific input text.

$$\pi_a(a|s, \mathcal{A}) = \pi_{pos}(a_{pos}|s, \mathcal{A}) \cdot \pi_{attr}(a_{attr}|s, \mathcal{A}) \quad (9)$$

Based on Eq. (8) and Eq. (9) we have

$$\begin{aligned} \pi(a|\mathcal{T}, \mathcal{H}, \mathcal{A}, o_t) &= \pi_s(s|\mathcal{T}, \mathcal{H}, o_t) \cdot \\ &\quad \pi_{pos}(a_{pos}|s, \mathcal{A}) \cdot \\ &\quad \pi_{attr}(a_{attr}|s, \mathcal{A}) \end{aligned} \quad (10)$$

It is easy for vision-based agents to learn the step inference policy  $\pi_s$ , as recent VLMs excel at image understanding and reasoning. Learning the non-positional inference policy  $\pi_{attr}$  is also manageable, since the non-positional aspects of an action can be directly inferred from the natural language step. For example, an action like "INPUT('Copenhagen')" can be directly inferred from a step such as "Input 'Copenhagen' into the arrival input box". The primary challenge lies in learning the positional sub-policy  $\pi_{pos}$  as discussed in Sec. 2. To address this challenge, we construct a large scale dataset focused primarily on grounding tasks to facilitate learning accurate positional actions.

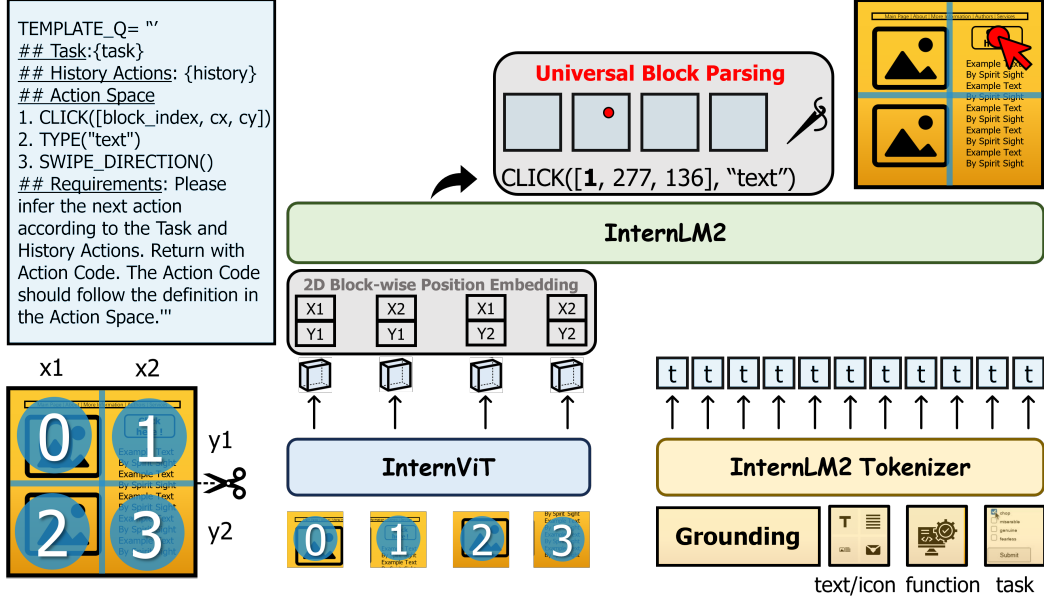


Figure 7. The overall architecture of SpiritSight. SpiritSight is pre-trained on GUI-Lasagne, a large-scale, multi-level, high quality GUI dataset. The UBP method solves the ambiguity in Dynamic High-Resolution input during model training.

### C. Overall Architecture

We build our model based on the pre-trained InternVL2, a family of advanced and open-sourced VLMs. We chose InternVL for the following reasons: (1) The large-scale and high-performance vision encoder is more capable to handle the text-rich GUI environment. (2) The dynamic resolution strategy largely preserves the details of the input screenshots, allowing for enhanced perception of fine-grained text and icon information. We take the advantage of large-scale InternViT with a large-scale GUI dataset described in Sec. 3. We further propose a Universal Block Parsing (UBP) method to resolve the ambiguity problem brought by dynamic resolution in Sec. 4.

The architecture of SpiritSight is depicted in Fig. 7. To begin with, the input image is the GUI screenshot. According to the dynamic resolution algorithm of InternVL, an appropriate ratio of input image is decided. Then, the image is divided into several blocks, each with a unique index, in preparation for the post-processing phase of our UBP method. These image blocks will be flattened into sequences before being sent to the vision encoder, which results in the loss of their 2D spatial relation. To address this problem, we introduce 2D Block-wise Position Embedding (2D-BPE) method, which maintains the blocks’ 2D spatial relation by adding a row embedding and column embedding to each block. Afterwards, the embedded image features, along with the task objective, the action space and the history actions are processed by the InternLM2 decoder to infer the action code. Finally, the action and corresponding coordinate for

operation is obtained by the UBP parser.

### D. Experiments

#### D.1. Implementation Details for Benchmark Experiments

We use InternVL2 (2B, 8B and 26B) [9, 25] as the base models and train them with two stages: continual pre-training and fine-tuning.

**Pre-training Stage.** We train all the GUI-Lasagne datasets mentioned in the Sec. 3 simultaneously. Different prompts are designed for different training tasks to avoid task confusion. See App. F for the detailed prompt content. We unfreeze the vision encoder, decoder, and MLP layer of InternVL. The learning rate is set to  $1e-4/1e-4/5e-5$  for InternVL-2B/8B/26B, respectively, and the batch size is set to 1024. We get **SpiritSight-Base** models after pre-training.

**Fine-tuning Stage.** We fine-tune SpiritSight-Base models in several downstream tasks separately. We define a distinct action space for each task to prevent action confusion. The max number of history actions is set to 5 to prevent excessive overload. For ScreenSpot benchmark, we follow the data proportions from Cheng et al. [11], using part of the level-1 and level-2 data of GUI-Lasagne, and the data from Deka et al. [12], Li et al. [33], Wang et al. [54] to train the entire model. For other GUI navigation benchmarks, we first train the entire model for 1 epoch using the level-3 data of GUI-Lasagne and the training data corresponding to each benchmark, then fine-tune the model for 1 epoch on the benchmark-specific training data using LoRA [21].

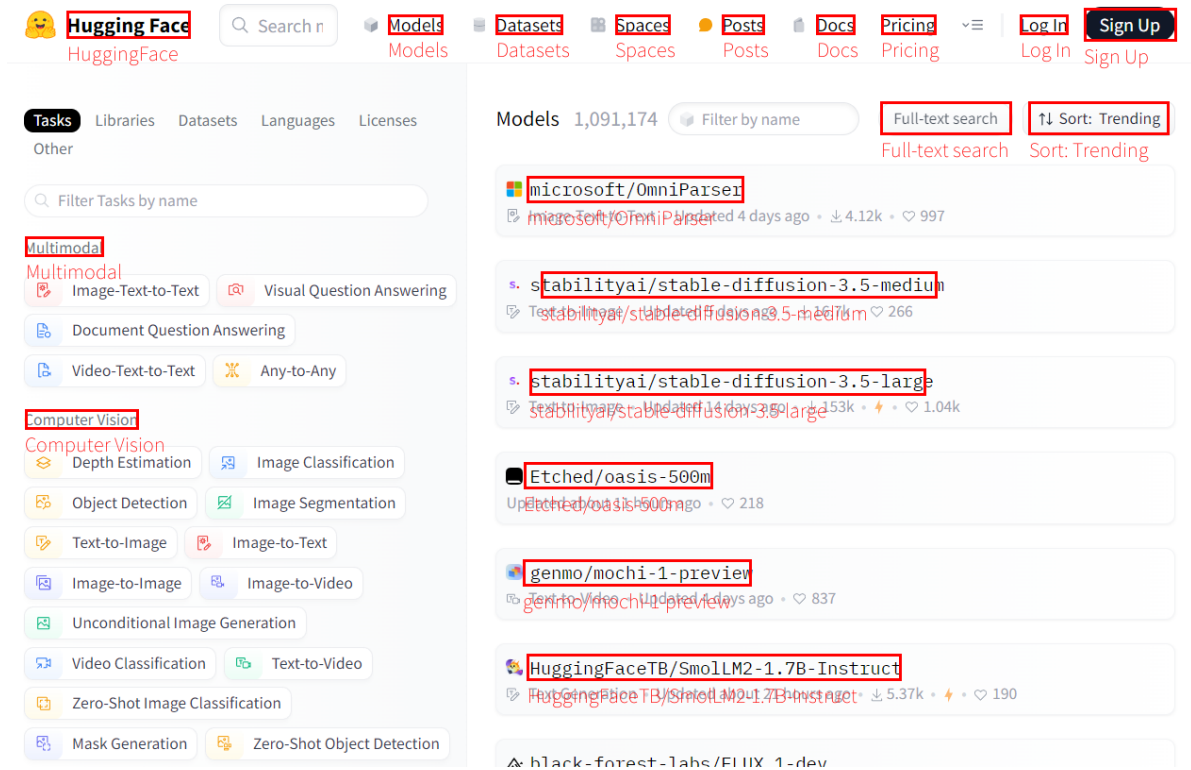


Figure 8. Visualization results of SpiritSight-2B on our custom text2bbox test set. The red boxes represent the generated results and the text next to it represent the text prompt.

While training the entire model, the learning rate is set to the same as pre-training, and the batch size is 1024. During fine-tuning, the learning rate is set to  $5e-5$ , the batch size is 64, with the alpha of vision encoder and LLM decoder set to 32 and 64, respectively.

## D.2. Implementation Details for Ablation Study

### Recognition and Grounding as Priors for GUI Navigation.

To verify the significance of the three levels of GUI-Lasagne data, we progressively removed level-3, level-2, and level-1 data from the training set during the pre-training stage and evaluate models on Multimodal-Mind2Web benchmark. During the fine-tuning stage, we train the SpiritSight-Base model only on the Multimodal-Mind2Web training data using LoRA, without training the whole models on level-3 data of GUI-Lasagne, as level-3 data is excluded from the pre-training datasets. The results are shown by the blue line in Fig. 6a.

We also conducted ablation experiments to evaluate the effectiveness of data cleaning and CoT construction strategies on the level-3 data, as shown by the orange line in Fig. 6a. We use the same setting as in the benchmark experiments, except with different versions of level-3 data (original version, data cleaning version and CoT version).

**Better Grounding Ability from UBP.** To verify the effectiveness of UBP on grounding task, we use LoRA for resource efficiency to fine-tune InternVL in 4 different settings (original as baseline, 2D-BPE, UBP, and 2D-BPE&UBP), respectively. First, We fine-tune InternVL1.5 (26B) on 10% of our GUI-Lasagne dataset. The alpha is set to 64. Then, we fine-tune the model on the Multimodal-Mind2Web training data. The alpha is set to 16 and 32 for vision encoder and LLM decoder, respectively.

**Scaling Effects on Dataset and Model Size.** We explore the impact of pre-training dataset and model size on SpiritSight using Multimodal-Mind2Web benchmark. The training strategies are same as in the benchmark experiments, except with different scale of pre-training data.

**Effective Transfer to other languages.** We split the training and test sets of GUIAct(web-multi) dataset into English and Chinese partitions, respectively. We fine-tune SpiritSight-Base (8B) on two sets of data: the entire training set (English&Chinese) and the English-only training set. Other training strategies are same as in the benchmark experiments.

Benchmarks	Platforms	Task	Metric	# Test Samples	History?
ScreenSpot[11]	Web, PC, Mobile	Functional Grounding	ClickAcc	1,272	×
Mind2Web[13]	Web	Navigation	Ele.Acc, Op.F1, Step SR	6,418	✓
AMEX[5]	Mobile	Navigation	AMS	5,284	✓
GUI-Odyssey[38]	Mobile	Navigation	AMS	29,426	✓
AndroidControl-High[32]	Mobile	Navigation	Step Accuracy	8,444	✓
AndroidControl-Low[32]	Mobile	Functional Grounding	Step Accuracy	8,444	×
GUIAct-Multi[7]	Web	Navigation	StepSR	1,065	✓
GUIAct-Single[7]	Web	Functional Grounding	StepSR	1,410	×

Table 5. Statistics of GUI benchmarks we include in this paper.

### D.3. Metrics

We use the metrics proposed in the corresponding benchmarks as shown in Tab. 5. Although they have different names, these metrics are similar: GUI grounding tasks consistently measure the hit rate of predicted bounding boxes, while GUI navigation tasks focus on single-step accuracy.

**Click Accuracy.** The proportion of test samples where the predicted location falls in the ground truth element bounding box.

**Element Accuracy (Ele.Acc).** Comparing the selected element with all acceptable elements. For vision-based methods, it is the same as Click Accuracy.

**Operation F1 (Op.F1).** Token-level F1 score for the predicted operation.

**Step Success Rate (Step SR) & Step Accuracy.** The proportion of successful steps. A step is regarded as successful only if both the selected element and the predicted operation are correct.

**Action Matching Score (AMS).** The proportion of predicted actions that match the ground-truth actions. Two actions can match if their action types are equal. For dual-point taps, they are considered equal if they fall within a 14% screen distance from each other. Alternatively, if the tap actions occur within the same detected bounding boxes, where the bounding boxes are augmented to 240% of their total size, they are considered equal. Finally, two dual-point scrolls are considered equal if they have the same primary scroll axis (vertical or horizontal).

### D.4. Grounding Abilities for GUI Visual Appearances

To evaluate the foundational ability of SpiritSight to ground visual appearance, we construct a small benchmark for text2bbox task. We random select a small number of URLs from those mentioned in Sec. 3.1. These URLs are not used in constructing the pre-training data. Following the method described in Sec. 3.1, we construct a test set with 3,700 text2bbox pairs. We adopt the hit rate as metric, defined to be the proportion of test samples where the model predicted

location falls within the ground-truth bounding boxes. Ultimately, SpiritSight-2B achieves a **96.1%** hit rate on this benchmark, demonstrating its strong capability in fundamental grounding tasks. Fig. 8 shows the visualization of the predicted bounding boxes from SpiritSight-2B.

## E. Data Collection

In this section, we present a cost-effective data collection strategy designed to construct a multi-level, large-scale and high-quality GUI dataset, called **GUI-Lasagne**. This dataset helps equip our models with robust abilities in GUI understanding, grounding, and navigation. The statistics of GUI-Lasagne are shown in Tab. 6 and Fig. 9.

### E.1. Level One: Visual-Text Alignment

We collected website URLs from two sources: the Common-Crawl [16] dataset and website rankings. We used the URLs from website rankings as a supplement to CommonCrawl due to its compromised quality, which includes a large proportion of blank pages, sparse-texted pages, and dead links. We then developed a data collection tool using playwright library to get real-world web data from the collected URLs.

For each URL, we navigate to the webpage and start data collection only after the webpage has fully loaded. We collect both the webpage screenshots and the corresponding DOM tree according to a carefully designed scheme. First, we perform grid sampling on the screen with a step size of 8 pixels. Then, we mark the element objects corresponding to the sampled points. Finally, we apply an HTML pruning algorithm to simplify the HTML code by retaining all the marked elements and their parent nodes. This process excludes elements that are small in size or invisible on the screen. Additionally, we label all the clickable elements by checking their pointer property and registered events. The resulting DOM trees are used to construct the bbox2dom pairs, while the element objects are utilized to create the text2bbox and bbox2text pairs.

After collecting data from the current website, we acquire new pages using two methods: scrolling down or clicking on

	Dataset	Platform	# Samples	# Tokens	# Elements	# Screenshots
DocVQA	Ureader-Instruction	General	489,150	23,356,600	489,150	118,355
	GUIChat	Web	50,832	14,789,523	50,832	17,979
	WebSRC	Web	23,742	162,177	23,742	5,462
	ScreenQA	Mobile	11,781	29,897	11,781	66,261 <sup>†</sup>
	RICO screen-captioning	Mobile	15,743	121,854	15,743	66,261 <sup>†</sup>
Level1	Web bbox2dom	Web	862,505	281,389,127	862,505	755,499 <sup>*</sup>
	Web text2bbox	Web	736,826	202,821,759	11,959,607	755,499 <sup>*</sup>
	Web bbox2text	Web	267,955	48,760,131	5,118,237	755,499 <sup>*</sup>
	AITW text2bbox	Mobile	1,058,638	309,594,824	27,993,054	1,276,752 <sup>‡</sup>
	RICO widget-captioning	Mobile	28,818	2,059,165	179,144	66,261 <sup>†</sup>
Level2	Web function2bbox	Web	906,087	156,273,895	9,710,488	755,499 <sup>*</sup>
	AITW function2bbox	Mobile	620,736	18,542,781	620,736	1,276,752 <sup>‡</sup>
	RICO-SCA	Mobile	18,148	2,485,239	145,517	66,261 <sup>†</sup>
Level3	AITW w/ CoT	Mobile	639,535	53,039,652	639,535	1,276,752 <sup>‡</sup>
Total			5,730,496	1,113,426,624	57,820,071	2,240,308

Table 6. Statistics of our GUI-Lasagne, a GUI continual pre-training dataset for our SpiritSight-Base Model. In the '# Screenshots' column, several datasets share the same suite of screenshot images, so numbers marked with the same superscript notation are counted only once.

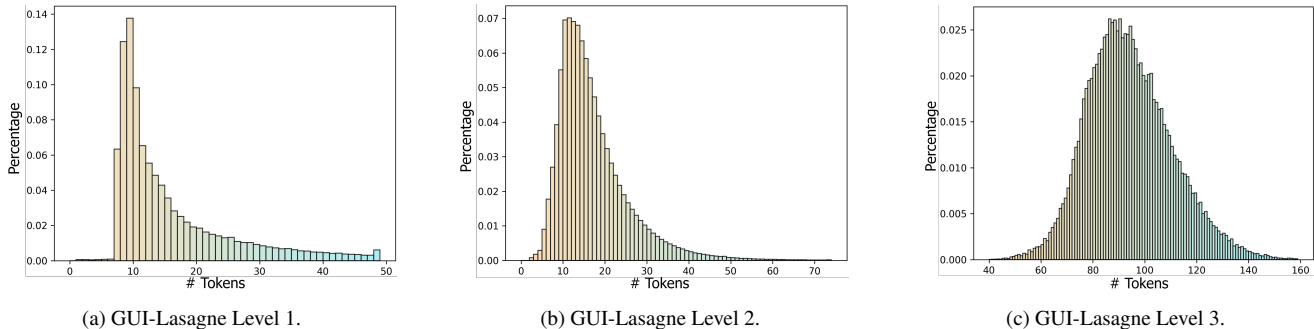


Figure 9. The distribution of token numbers of our GUI-Lasagne dataset for GUI continual pretraining.

an element, with these choices being randomly sampled. If clicking on an element is chosen, the target element is also randomly sampled from all clickable elements. We collect a maximum of 30 pages for each URL. We repeat the above mentioned process to achieve an automated data collection. Ultimately, we collect 755K webpage screenshots along with their DOM trees, where English samples account for 3/4 of the data and Chinese samples account for 1/4.

## E.2. Level Two: Visual-Text Alignment

We leverage InternVL’s image understanding capabilities to collect function grounding data. Specifically, we divide each screenshot into a 3x3 grid and describe the approximate location of the target element in text format (*e.g.* in the top-left corner of the image). Additionally, We place a bounding box around the target element in the screenshot to precisely specify its location. To prevent color confusion,

we dynamically determine the color of the bounding box. First, we analyze the color data around the target element, then select the most visually prominent color among red, green, and blue as the color of bounding box. By providing InternVL2-26B with the screenshot, the element’s text content or icon caption, and the location description, we prompt it to generate the function of the target element. Additionally, we utilize InternLM2.5-20B to enhance the quality and diversity of the generated function descriptions. The two prompts are shown in App. G.2.

A validation is performed by two experienced human annotators. Specifically, we randomly sampled 100 images from the collected data to create a human evaluation set, with the functional description of all labeled element. The annotators are asked to determine whether the functional description is correct. A functional description is considered acceptable if the corresponding element can be uniquely



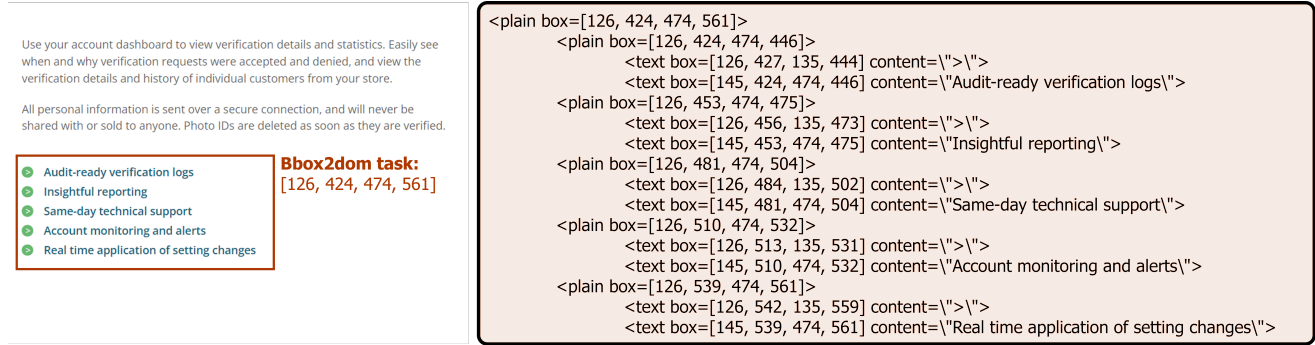


Figure 10. An example of the Bbox2dom task. Left shows a given bounding box on a web page, right shows its corresponding simplified DOM structure.

identified in the screenshot based on the description. We calculate the proportion of acceptable functional descriptions out of the total descriptions. Ultimately, the human evaluation achieves an acceptance rate of 90.9%, indicating the effectiveness of our data synthesis strategy. We show some evaluation examples in Fig. 11.

### E.3. Level Three: Visual GUI Navigation

We utilize the public available AitW [46] dataset to construct our GUI navigation training data. AitW is a large-scale mobile navigation dataset where each screenshot is labeled with the corresponding goal, the current step, *etc.* We select the all general, install and web-shopping sets and 1M samples of google-apps set as the source data. We discard the single set as the screenshots are duplicated with others. However, AitW involves a certain amount of incorrectly labeled samples as mentioned by AitZ [72] and AMEX [5].

We clean the AitW [46] dataset with GPT-4o and adopt Chain-of-Thought (CoT) [60] to make the judgment more accurate. Specifically, for non-final steps, we prompt GPT-4o with the task description, the current action annotation, two screenshots at the current and the next steps, respectively. GPT-4o is then instructed to first summarize the two screenshots and identify the differences between them, then describe the current step based on these differences, and finally assess the reasonableness of the current action annotation. We filter out steps identified as unreasonable by GPT-4o. For the final step, we prompt GPT-4o with the task description and the current screenshot. It is then instructed to summarize the screenshot and determine whether the task was successfully completed. We filter out the final steps considered successfully completed. Note that we only discard the steps that do not meet the requirements, and do not discard the entire trajectories. The prompts for GPT-4o are shown in App. G.3. The collected data examples are shown in Fig. 11. Ultimately, we obtain 0.63M CoT-style GUI navigation training samples from 1.48M source samples after cleaning.

We also perform a validation for level-3 data by two experienced human annotators. Specifically, We randomly sampled 100 steps that considered as reasonable (the Cleaned Set) and 100 discarded steps by GPT-4o (the Discarded Set). For each step sample, the annotators are provided with the screenshots, the overall task description, and the validity judgments generated by GPT-4o. Then they are asked to determine whether the results of GPT-4o is correct. We report the true positive rate (TPR) for the Cleaned Set and the true negative rate (TNR) for the Discarded Set. The Cleaned Set achieved a TPR of 93.7%, indicating the reliability of our data cleaning procedure. The Discarded Set achieved a TNR of 76.3%. Though the result is not as high, it is unrelated to the quality of our dataset. In the future, we will explore a more efficient data cleaning method to improve the TNR while keeping the TPR approximately unchanged.

### F. Training Data Format

We constructed a large scale dataset for GUI continual pre-training, including text2bbox, bbox2text, bbox2dom, and function2bbox tasks. To make sufficient use of the context length of the model, we pack multiple data pairs in each training sample for text2bbox, bbox2text and function2bbox tasks, and select the box that includes as many elements as possible for bbox2dom task. We use the center point, width and height to represent a bounding box. It is worth noting that, aside from the function2bbox task, we add an additional block index to each bounding box, which is derived from our proposed UBP method. For function2bbox task, we use the original global coordinate system as the bounding boxes are too large to be considered a point and grounding is not the main focus of this task. Additionally, we normalize all coordinate values between 0 and 999 and round them to the nearest integer. Below are the training data templates for each task. Notably, the prompt is randomly selected from a pool during data construction. See App. G.1 for details of the prompt pool.

### **Data Format for text2bbox Task**

*user:*

<image>

1.{text 1}

2.{text 2}

3.{text 3}

...

Provide the bounding boxes of each given text in a list format.

*assistant:*

1.{{block-index, cx, cy, w, h}}

2.{{block-index, cx, cy, w, h}}

3.{{block-index, cx, cy, w, h}}

...

### **Data Format for function2bbox Task**

*user:*

<image>

1.{function description 1}

2.{function description 2}

3.{function description 3}

...

In this image from a webpage, find out where to click for a certain need and provide bbox coordinates in a list format.

*assistant*

1.{{block-index, cx, cy, w, h}}

2.{{block-index, cx, cy, w, h}}

3.{{block-index, cx, cy, w, h}}

...

### **Data Format for bbox2text Task**

*user:*

<image>

1.{{block-index, cx, cy, w, h}}

2.{{block-index, cx, cy, w, h}}

3.{{block-index, cx, cy, w, h}}

...

Provide the text content of each given bounding box in a list format.

*assistant:*

1.{text 1}

2.{text 2}

3.{text 3}

...

### **Data Format for bbox2dom Task**

*user:*

<image>

I'd like some information about the specific region [cx, cy, w, h] in the image.

*assistant:*

{DOM\_Tree}

## **G. Prompt Templates**

### **G.1. Evaluation Inference**

#### **Prompt for Evaluation Inference**

## Task: {task}

## History Actions:

{history}

## Action Space

{Action Space}

## Requirements: Please infer the next action according to the Task and History Actions.

Return with Action Code. The Action Code should follow the definition in the Action Space.

### **G.2. Level-two Function Generation**

#### **Prompt for Level-two Function Generation**

Please infer the purpose of the operation "click on the '{text}' on the {region} of the webpage" based on the webpage.

Please deliver the purpose specifically and clearly, which points to the certain item.

Its direct context includes the following information: {context\_text}.

Please make the answer only in English.

Let's think step by step.

Your final answer should be in a new line and included in double quotation like:

The purpose is "xxx".

**Prompt for Level-two Function Augmentation**

Can you rewrite the original purpose "{purpose}" into a short phrase?

Here are some examples:

{Few-shot example 1 }

{Few-shot example 2 }

{Few-shot example 3 }

Output only the refined purpose, start with 'to', without any explanation.

**Prompt for Level-three Last Step Data Processing**

Task: {task}

Action History: {history}

You have just completed a mobile task with a series of actions listed in Action History. The picture shows the final screen of the mobile.

Return:

1. Summarize the picture about its main content and its functionality. Describe it with necessary details, but not too long.
2. Analyze if the task is successfully completed from the perspectives of success and completion separately.
3. Return the final answer of the analysis with just 'True' or 'False'.

### G.3. Level-three Data Processing

**System Prompt for Level-three Data Processing**

You are a mobile operation assistant, the main goal is to help identify whether the mobile navigation operation is correct.

**Prompt for Level-three Middle Step Data Processing**

Task: {task}

Action History: {history}

The Current Action: {action}

You are completing a mobile task and now in step {step\_idx}. Picture 1 shows the current screen with action demonstration and picture 2 shows the screen after performing The Current Action on picture 1. You are also given the Action History before the Current Action.

Return:

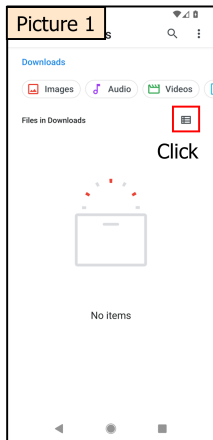
1. Summarize picture 1 about its main content and its functionality. Also describe the changes that have occurred in Figure 2 compared to Figure 1. Describe them with necessary details, but not too long.
2. Based on the changes between Figure 1 and Figure 2, estimate the function of the Current Action. Return with format of "The function of the Current Action: xxx"
3. Analyze the rationality of the Current Action based on the Task. Return only the reason.
4. Return the final answer of the rationality of the Current Action with just 'True' or 'False'.
5. Analyze if the Task is successfully completed. Return only the reason.
6. Return the final answer of the complementarity of the Task with just 'True' or 'False'.



- 1:  To provide daily temperature and forecast with activity and outfit suggestions.
- 2:  To provide a list of recommended outdoor activities based on the current weather conditions in Victoria, BC.
- 3:  To recommend appropriate clothing attire based on the current weather conditions.
- 4:  To get tailored morning run advice
- 5:  To obtain personalized advice on the optimal timing for walking activities.
- 6:  To view the weather forecast for the full 72 hours
- 7:  To access detailed weather for a specific time
- 8:  To view the hourly weather forecast for Victoria, BC at 4am.
- 9:  To check the weather forecast for 5am in Victoria, BC
- 10:  To access more detailed weather information for the specific time slot of "6am".
- 11:  To view detailed weather information for the 7 a.m. hour in Victoria, BC



- 1:  To switch the language of the webpage to Spanish
- 2:  To switch the language of the webpage from Spanish to English
- 3:  To change the language of the webpage to Catalan
- 4:  To navigate to the main page of the Universitat de Lleida Valorització
- 5:  To access the contact page for the University of Leiden's Valorization & Technology Transfer Office.
- 6:  To access historical content or archived data from the specified date and time.
- 7:  To access more information about the 500,000 euros grant from FEDER funds received by the UdL Technology Transfer and Valorization Unit to promote technological development, innovation, and quality research.

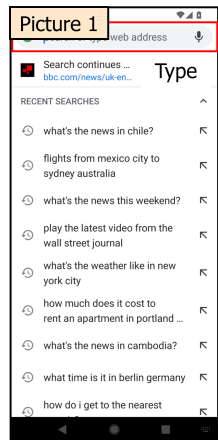


**"task":**  
Open the downloads

**"action":**  
Click(0.88, 0.25)

**"rationale":** False

**Action reason:**  
The Current Action is not rational based on the Task because the task is to open the downloads, not to change the view mode.

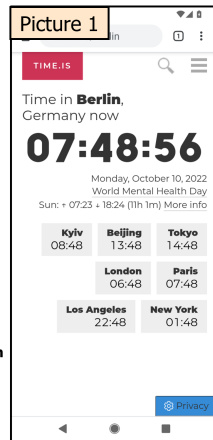


**"task":**  
What's the news in Malaysia?

**"action":**  
Type("What's the news in Malaysia?")

**"rationale":** True

**Action reason:**  
The Current Action is rational because it directly addresses the task of finding out the news in Malaysia by initiating a relevant search query.



**"task":**  
What time is it in Berlin?

**"complete":**  
True

**Action reason:**  
The Current Action is rational because it aims to bring back the main content that shows the time in Berlin, which is the information needed to complete the task.

Figure 11. The examples of our collected GUI function and navigation data. The upper two screenshots show the functional annotation generated by InternVL2 and InternLM2.5. The lower three samples show the judgment results and reasons provided by GPT-4o.